Brazilian Journal
of Chemical
Engineering

ISSN 0104-6632
Printed in Brazil
www.abeq.org.br/bjche

Vol. 30, No. 03, pp. 589 - 597, July - September, 2013

PREPARATION, CHARACTERIZATION AND GAS PERMEATION STUDY OF PSf/MgO NANOCOMPOSITE MEMBRANE

S. M. Momeni and M. Pakizeh*

Chemical Engineering Department, Faculty of Engineering, Ferdowsi University of Mashhad,
Mashhad, P.O. Box 91775-1111, Iran.
E-mail: pakizeh@um.ac.ir

(Submitted: June 3, 2012 ; Revised: August 13, 2012 ; Accepted: September 22, 2012)

Abstract - Nanocomposite membranes composed of polymer and inorganic nanoparticles are a novel method to enhance gas separation performance. In this study, membranes were fabricated from polysulfone (PSf) containing magnesium oxide (MgO) nanoparticles and gas permeation properties of the resulting membranes were investigated. Membranes were prepared by solution blending and phase inversion methods. Morphology of the membranes, void formations, MgO distribution and aggregates were observed by SEM analysis. Furthermore, thermal stability, residual solvent in the membrane film and structural ruination of membranes were analyzed by thermal gravimetric analysis (TGA). The effects of MgO nanoparticles on the glass transition temperature (T_g) of the prepared nanocomposites were studied by differential scanning calorimetry (DSC). The T_g of nanocomposite membranes increased with MgO loading. Fourier transform infrared (FTIR) spectra of nanocomposite membranes were analyzed to identify the variations of the bonds. The results obtained from gas permeation experiments with a constant pressure setup showed that adding MgO nanoparticles to the polymeric membrane structure increased the permeability of the membranes. At 30 wt% MgO loading, the CO_2 permeability was enhanced from 25.75×10^{-16} to 47.12×10^{-16} mol.m/(m^2.s.Pa) and the CO_2/CH_4 selectivity decreased from 30.84 to 25.65 when compared with pure PSf. For H_2, the permeability was enhanced from 44.05×10^{-16} to 67.3×10^{-16} mol.m/(m^2.s.Pa), whereas the H_2/N_2 selectivity decreased from 47.11 to 33.58.
Keywords: Nanocomposite membranes; Polysulfone; Gas permeation; MgO nanoparticles.

INTRODUCTION

Membrane technology is a separation process used in many chemical industries. Some of the main benefits of membrane technology in comparison with other separation technologies are: low processing costs, convenience processing, low energy need and environmental regulations (Koros and Fleming, 1993; Pandey and Chauhan, 2001).

Membranes are divided into polymeric and inorganic membranes. Polymeric membranes, as opposed to inorganic ones, are widely used in gas and liquid separation due to their advantages such as ease of preparation, flexibility and other desirable properties (Maier, 1998; George and Thomas, 2001; Freeman and Pinnau, 1999). Robeson (1991) revealed that, even though these advantages exist, polymeric membranes still suffer from a trade-off between gas permeability and selectivity. To overcome this problem, nanocomposite membranes have been considered for gas separation. Nanocomposite membranes consist of polymeric material as the continuous base phase and inorganic materials dispersed in the polymeric phase. Desirable properties of nanocomposite membranes are due to the appropriate combination of polymer and inorganic

*To whom correspondence should be addressed

materials. For instance, nanocomposite membranes have the desirable flexibility and processability of polymers and the selectivity and thermal permanence of inorganic materials (Chung *et al*., 2007; Morooka and Kusakabe, 1999; Joly *et al*., 1999; Suzuki and Yamada, 2005; Okui *et al*., 1995).

Inorganic materials used for the preparation of nanocomposite membranes have various properties and structure. In one classification, inorganic particles can be categorized as porous and nonporous fillers. These materials, when loaded in the polymeric matrix, exhibit various transport mechanisms. Zeolites, carbon molecular sieves (CMS) and metal oxides are various types of inorganic materials that are widely used in the preparation of nanocomposite membranes. These fillers provide great performance for gas separation processes (Te Hennepe, 1998; Suda and Haraya, 1997; Moaddeb and Koros, 1997; Hu *et al*., 1997).

One of the main glassy polymers commonly used in membrane technology is polysulfone (PSf). PSf has good thermo-mechanical strength and gas separation properties. It is also cost effective and has high resistance to plasticization, which makes it a good candidate for membrane development (Rafiq *et al*., 2012). Different gas permeation properties of PSf have been widely studied for gas separation processes (Zimmerman *et al*., 1997). Several studies have focused on the presence of nanofillers in polymer-based membranes.

Ahn *et al*. (2008) studied the effect of silica nanoparticles on the gas separation performance of polysulfone membranes. They obtained a significant increase in permeability of O_2 and CH_4. The O_2 permeability of PSf/silica membranes was increased four times over pure PSf and CH_4 permeability was five times greater than for PSf. They also reported that the H_2/CH_4 and H_2/CO_2 selectivities decreased from 53.6 and 1.87 in pure PSf to 29.36 and 1.64 in 20% wt. silica nanocomposite membranes, respectively (Ahn *et al*., 2008).

Kim *et al*. (2008) studied the effect of mesoporous MCM-41 on the gas permeability of PSf membranes. At 40 wt.% loading, the O_2/N_2 selectivity decreased from 5 to 4 and the CO_2/CH_4 selectivity decreased from 23 to 15, while the O_2 and CO_2 permeability increased from 0.98 to 3.4 barrer and 4.5 to 14.8 barrer, respectively.

Hosseini *et al*. (2007) prepared Matrimid membranes embedded with porous MgO nanoparticles. The addition of MgO nanoparticles led to an increase in gas permeability of the polyimide membrane. The highest permeability occured in membranes containing 40 wt% MgO loading. At this loading, the O_2 permeability was enhanced from 1.9 to 3.4 barrer and the O_2/N_2 selectivity decreased from 7.14 to 6.5. For CO_2, the permeability was enhanced from 6.8 to 9.9 barrer, whereas the CO_2/CH_4 selectivity decreased from 33.3 to 26.4. However, the selectivity of nanocomposite membranes was less than that of neat Matrimid. The results illustrate that pore dimensions of MgO nanoparticles are larger than the size range of gas molecules (Hosseini *et al*., 2007).

This study reports the influence of MgO nanoparticles on the structural characteristics and the gas permeability of PSf polymer membranes. MgO is one of the metal oxides used for enhancing strength and thermal resistance of membranes. It also exhibits good affinity for some gas molecules and can be used as a potential metal oxide filler in nanocomposite gas separation membrane preparation (Han *et al*., 2012; Hosseini *et al*., 2007). Nanocomposite membranes were fabricated by the solution-casting method with different loadings of MgO nanoparticles. Particle dispersion and morphology of the prepared nanocomposite were characterized using Scanning Electron Microscopy (SEM). Characteristics of membranes such as thermal degradation and glass transition temperature (T_g) were evaluated by TGA and DSC. Gas permeation properties of CO_2, CH_4, N_2, and H_2 are reported as a function of particle concentration.

THEORY

Gas Transport

Gas transport of nonporous dense polymeric membranes is based on the solution-diffusion mechanism (Matteucci *et al*., 2008):

$$P = \frac{N.L}{p_2 - p_1} \tag{1}$$

$$P = D.S \tag{2}$$

where P is the gas permeability, N is the steady-state permeation flux, L is the film thickness, p_1 and p_2 are the gas pressures at the permeate and retentate sides, respectively, D is the effective concentration diffusivity and S is the solubility coefficient (Matteucci *et al*., 2006). The ability of a polymer to separate two components is often characterized in terms of the ideal selectivity, $\alpha_{A/B}$, which is the ratio of permeability of the two components:

$$\alpha_{A/B} = \frac{P_A}{P_B} \tag{3}$$

where P_A and P_B are the permeability coefficients of gases A and B (Pollo *et al*., 2012).

EXPERIMENTAL

Materials

Polysulfone (Ultrason6010) was purchased from BASF Company. PSf is a glassy polymer with a glass transition temperature (T_g) of 189 °C. The reported density of PSf is 1.24 g/cm^3. Figure 1 shows the repeat unit of PSf. Dimethylacetamide (DMAc) was provided from Merck Company. Spherical MgO nonporous nanoparticles were kindly supplied by PlasmaChem, Germany. According to the manufacturer, MgO had a crystalline density of 3.58 g/cm^3 and a particle diameter of 20 nm. The BET surface area was reported to be 50 m^2/g.

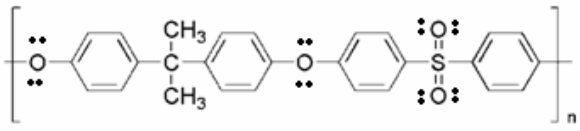

Figure 1: Repeating unit of PSf.

Membrane Preparation

In this study membranes were prepared by the immersion precipitation technique. Immersion precipitation is a simple way to fabricate polymer – inorganic nanocomposite membranes. This method is convenient and suitable because the concentrations of polymer and inorganic fillers are controlled easily. Aggregation of nanofillers in membranes is a problem of this method (Cong *et al*., 2007; Stephan *et al*., 2006; Mascia *et al*., 1996; Shi *et al*., 2000). The MgO content used in the membranes was calculated as the volume fraction Φ_f by:

$$\phi_f = \frac{w_f / \rho_f}{\left(w_p / \rho_p + w_f / \rho_f \right)} \quad (4)$$

where w_f and w_p refer to the weight of filler and polymer, respectively and ρ_f and ρ_p are the density of filler and polymer, respectively (Ahn *et al*., 2008; Matteucci *et al*., 2008). Prior to preparing the sample solutions, all glassware, MgO powder and polysulfone were dried in an oven at 60 °C for 2 hours and allowed to cool to room temperature to reduce the introduction of adventitious water.

Preparation of Polysulfone Membranes

Polysulfone solution was prepared by dissolving 15 wt% of polysulfone in DMAc under continuous stirring for 24 hours at 30 °C until the polymer dissolved. Ten minutes before casting, the mixture was sonicated. Then PSf films were cast on a clean, dry, level glass plate and after 1 minute evaporating time, membranes were immersed in a water coagulation bath (20 °C) for 24 hr. Finally membranes were dried in an oven at 70 °C about 6 hours to remove the remained solvent and water from the coagulation bath.

Preparation of PSf/MgO Nanocomposite Membranes

The nanocomposite membranes where prepared by addition of MgO nanoparticles in different loadings to the polymer solution. First MgO nanopowder was dispersed in DMAc under continuous stirring for about 3 hours followed by sonication for 5 min to break up any aggregation and improve the dispersion quality. Then polymer was gradually added up to 15 wt% concentration and the stirring was continued for 24 hours to achieve a homogenous solution. After that, membranes were cast in the same way as for pure PSf membranes. The MgO content (Φ_f) in the nanocomposite was calculated by Eq. (4). Table 1 shows the amount of MgO in the prepared nanocomposite membrane.

Table 1: Sample designations of membranes and their MgO contents.

Membrane name	Weight fraction of MgO(%)
PSf - 0	0
PSf - 10	10
PSf - 20	20
PSf - 30	30

Morphology Characterization

The morphologies of pure PSf and PSf/MgO nanocomposite membranes were observed by scanning electron microscopy (SEM). The samples were fractured in liquid nitrogen. The samples were then examined using a LEO-VP1450 scanning electron microscope equipped with an element energy dispersive X-ray (EDX) spectrometer and image capturing software. All photos were taken using an accelerating voltage of 30 kv.

FTIR and Thermal Stability Tests

The variation of bonds due to incorporation of MgO nanoparticles into the prepared membranes was investigated by Fourier transfer infrared (FTIR) spectroscopy. A Bruker Equinox 55 in the range of 400 to 4000 cm^{-1} was used for this analysis. In order to investigate the thermal degradation, the prepared membranes were analyzed by thermal gravimetric analysis (TGA) on a Shimadzu TGA-50. The sample was heated from 25 to 1000 °C at the rate of 10 °C/min.

The glass transition temperature (T_g) of prepared membranes was obtained by differential scanning calorimetry (DSC) with a Linseis PT-1600. The samples were heated from 25 to 300 °C at a heating rate of 10 °C/min, under a nitrogen atmosphere.

Gas Permeation Measurements

Permeation tests of pure gases (H_2, N_2, CH_4 and CO_2) in PSf and PSf/MgO membranes were carried out by a constant pressure method (Matteucci *et al*., 2008; Stern *et al*., 1963). The film was displayed to the test gases and the data were collected from the steady-state permeate flow rate through a bubble flow meter. A schematic of experimental set-up is presented in Figure 2. Each test was repeated 3 times and the average value presented.

The gas permeability was calculated according to the following equation (Merkel *et al*., 2000):

$$P = \frac{L}{A(p_2 - p_1)}Q \quad (5)$$

where l is the film thickness (m), Q is the permeate volumetric flow rate (mol/s), p_2 is the feed absolute pressure, p_1 is the downstream absolute pressure (Pa) and A is the membrane area available for transport (m^2). All experiments were performed at atmospheric downstream pressure (permeate). Permeability is reported in units of (mol. m /(m^2.s.Pa)).

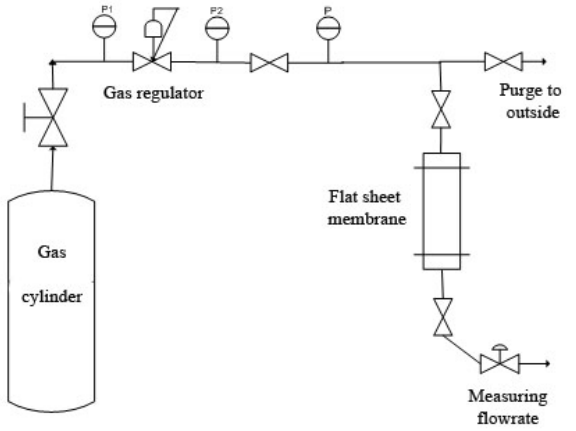

Figure 2: Schematic of experimental set-up used for gas permeation tests.

RESULTS AND DISCUSSION

Morphology of PSf/MgO Nanocomposite Membranes

By SEM analysis, the presence and distribution of MgO nanoparticles and the morphology of nanocomposite membranes was observed. Cross-sections of the resulting membranes were prepared by freeze-fracturing the membranes after several minutes immersion in liquid N_2. Then cross sections of the prepared membranes were subjected to SEM analysis and the picture captured. Figure 3 shows the cross sectional SEM images of a pure PSf membrane and 30 wt% MgO in PSf. In this figure, it can be seen that the prepared membranes are porous with a thin dense layer. Particle distribution and agglomeration can be seen in Figure 3(b). In Figure 4, we can observe the distribution of MgO particles in prepared membranes from a top view. Figure 5 shows a uniform distribution of MgO nanoparticles inside the polymer matrix analyzed by EDX. It can be seen clearly in these figures that the distribution, content and agglomeration of particles increased with weight fraction of MgO.

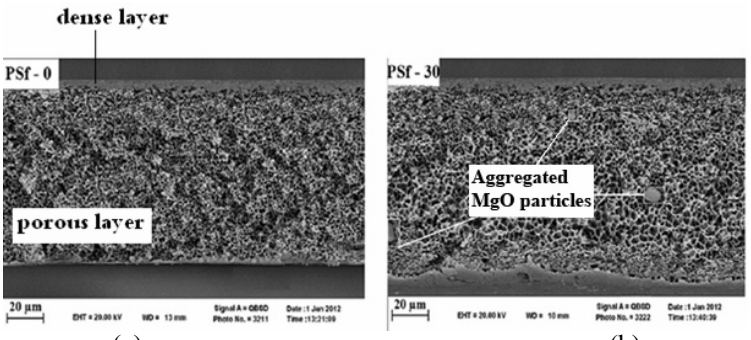

(a) (b)

Figure 3: (a) Cross sections of pure PSf membrane and (b) PSf-30 nanocomposite membrane.

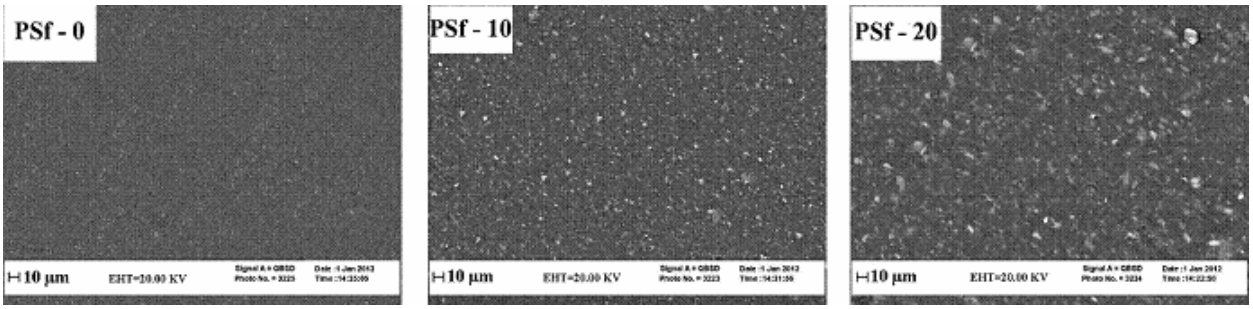

Figure 4: SEM of a top view of pure PSf membrane and PSf-10, PSf- 20 nanocomposite membranes.

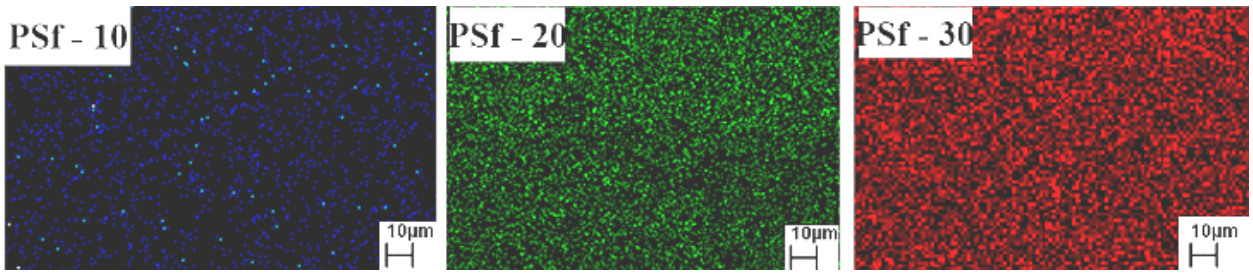

Figure 5: Distribution of MgO particles in the PSf polymer matrix, by SEM-map (EDX).

FTIR and Thermal Stability Tests

Structural characterization of the pure PSf membrane and the PSf/MgO nanocomposite membranes was investigated by FTIR, TGA and DSC analyses. Figure 6 shows the FTIR spectra of the MgO powder, pure PSf and nanocomposite PSf membranes. In the spectra of MgO powder, the broad absorption band at 488 cm^{-1} associated with the symmetric Mg=O bond can be observed. The absorption bands at 3461 cm^{-1} (stretching) and 1490 cm^{-1} (bending) indicate the presence of hydroxyl groups (OH), which is due to available humidity on the MgO surface or absorbed moisture by the KBr matrix used for the FTIR measurements (Gu *et al*., 2004). The bands of the MgO powder were observed clearly in the nanocomposite membranes PSf-10 and PSf-20.

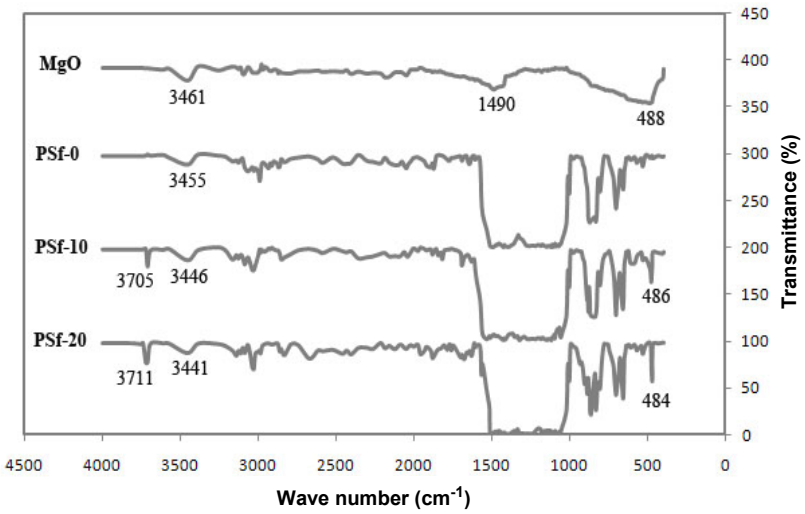

Figure 6: The FTIR spectra of MgO, PSf and PSf/MgO membranes.

In spectra of the nanocomposite membranes (PSf-10 and PSf-20), we can observe that, upon increasing the nanofiller, the absorption band of symmetric Mg=O appears with greater strength and lower frequency. The absorption bands around 3400-3500 cm^{-1} are related to OH groups, which can be due to residual water from the coagulation bath or available humidity. Moreover, in spectra of PSf-10 and PSf-20 we can observe an absorption band around 3700 cm^{-1} due to the Mg-OH bond (Pavia, 1997; Hsu and Nacu, 2005).

The thermal properties of unfilled PSf and MgO-filled PSf membranes were characterized by TGA and DSC analysis to verify the effect of MgO nanoparticles on the polymer chain stiffness. The thermal stabilities as a function of weight (%) were evaluated via TGA with a heating rate of 10 ºC/min (Figure 7). It can be observed that the degradation of all membranes occurs in three steps.

The first step, from room temperature (25 °C) to 280 °C, illustrates the removal of the volatile matter and the evaporation of residual solvent and absorbed water. The second step, from 280 °C to 480 °C, represents the main thermal degradation of the polymer chains. The third step, starting at 480 °C, demonstrates the carbonization of the degraded products. The onset point of decomposition is about 280 °C as shown in Figure 6 (Arthanareeswaran *et al*., 2004; Chatterjee and Conrad, 1968).

Differential scanning calorimetry (DSC) was performed to study the changes in the glass transition temperature (T_g). Mechanical, thermal and operating history of the sample strongly affect the glass transition temperature (T_g) (Ahn *et al*., 2008; Moore and koros, 2005). The DSC thermograph for the PSf and PSf/MgO nanocomposite membranes are shown in Figure 8. The T_g of PSf is typically reported as 189 °C (Ahn *et al*., 2008; Kim and Cho, 2011).

Increased T_g reflects the variation in long-range mobility of polymer chains (Moaddeb and koros, 1997; Ahn *et al*., 2008). It can be said that, due to the low mobility of MgO and higher stiffness of these particles, the mobility of the polymer chains would decrease and the T_g of nanocomposite membranes would increase.

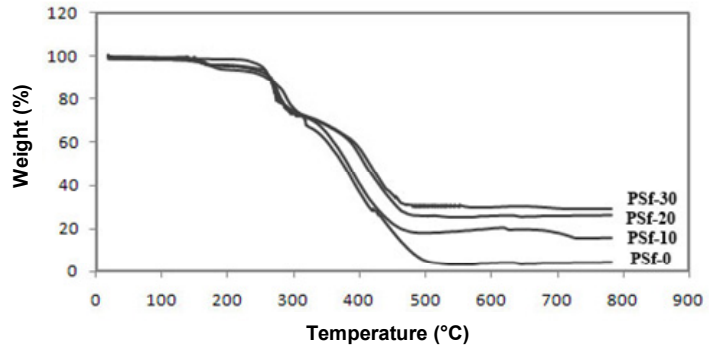

Figure 7: TGA curves of PSf membrane and PSf/MgO nanocomposites.

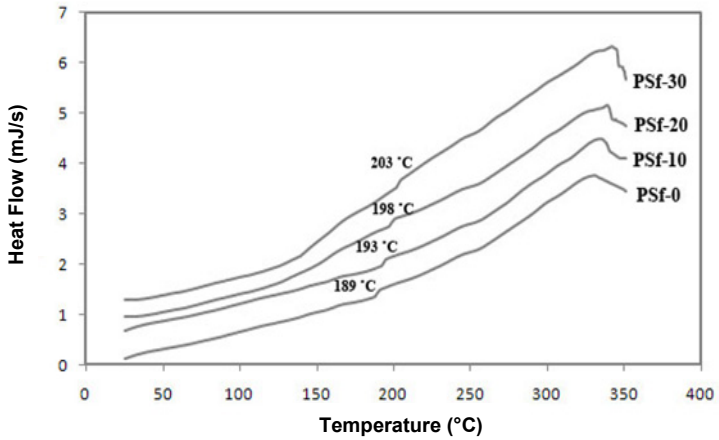

Figure 8: DSC thermograms of the PSf and PSf/MgO nanocomposite membranes.

Gas Permeation Results

The permeation of N_2, CH_4, H_2 and CO_2 in pure PSf and PSf/MgO nanocomposite membranes was investigated at ambient temperature and pressure of 4×10^5 Pa. The results of gas permeation properties of nanocomposite membranes are illustrated in Table 2 and Figure 9. As shown in this table, the permeability of carbon dioxide increases from 25.75×10^{-16} to 47.12×10^{-16} mol.m/(m^2.s.Pa) and the permeability of hydrogen and nitrogen increase from 44.05×10^{-16} and 0.93×10^{-16} to 67.30×10^{-16} and 2.00×10^{-16} mol.m/(m^2.s.Pa), respectively. By comparison of our results with targeted papers (Ahn *et al*., 2008; Kim *et al*., 2008), we can see that the membranes prepared achieved convenient results.

Gas solubility, gas molecular size, void volume in the polymer and also the mobility of the polymer chains are the main properties of polymeric membranes that affect the permeability of gases through the polymer. In the glassy polymers such as PSf, due to their rigid structure and the vacancy of chain mobility, the permeation of the gases in the polymer is defined by the diffusivity ability of the gases in the polymer (Tin *et al*., 2003; Tsujita, 2003).

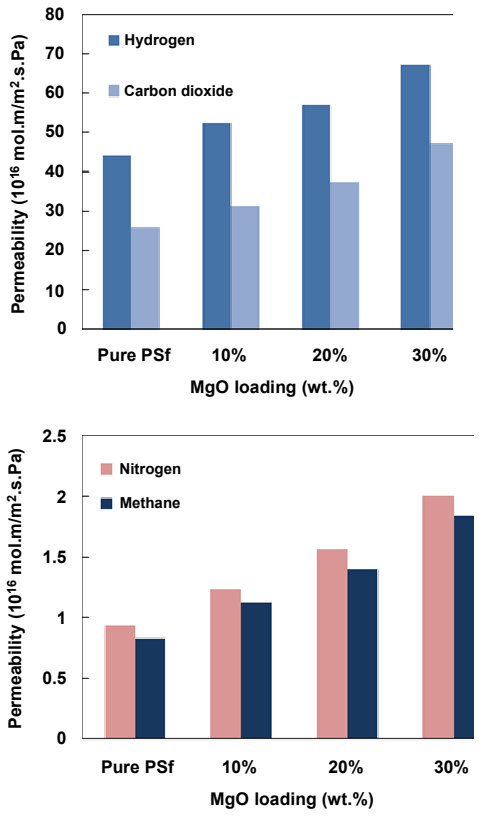

Figure 9: The comparison of gas permeability for nanocomposite membranes.

Generally, incorporation of nanoparticles in a glassy polymer matrix can disrupt its chain packing, which increases the free volume in the polymer phase. In addition, voids at the polymer-particle interface or between particles in particle aggregates result in an increase in total free volume. Increased total free volume leads to increases in diffusion and solubility coefficients and thus causes gas permeability to be greater in nanocomposites than in pure polymer. In nanocomposite PSf/MgO membranes, nonporous MgO nanoparticles substitute some portions of the dense and porous structure of the polymer matrix. It can be also observed from the SEM that voids have been formed at the polymer-MgO interface. Table 2 presents the gas permeability of pure PSf and nanocomposite membranes. As can be seen in Table 2, by increasing MgO loading, gas permeability increases. This trend is similar to those reported for a variety of non-porous nanoparticle fillers dispersed in glassy polymers.

The separation performance of membranes was calculated for selected gas pairs. The ideal gas selectivities of MgO-filled membranes are listed in Table 3.

Table 2: Gas permeabilities of PSf and PSf/MgO nanocomposite membranes as a function of MgO at ambient temperature and 4 bar.

Membrane name	Permeability ($\times10^{-16}$ mol.m/m^2.s.Pa)			
	H_2	CO_2	N_2	CH_4
PSf - 0	44.05 ± 4.50	25.75 ± 1.53	0.93 ± 0.16	0.83 ± 0.16
PSf - 10	52.27 ± 4.07	31.29 ± 1.73	1.23 ± 0.13	1.13 ± 0.10
PSf - 20	56.88 ± 3.80	37.50 ± 1.63	1.56 ± 0.16	1.40 ± 0.13
PSf - 30	67.30 ± 5.04	47.12 ± 1.77	2.00 ± 0.13	1.83 ± 0.13

$$1\ \text{barrer} = 3.34\times10^{-16}\left(\text{mol.m}/\text{m}^2\text{.s.Pa}\right)$$

Table 3: The ideal selectivity of pure PSf and PSf–MgO nanocomposite membranes with different MgO loadings.

Membrane name	Ideal Selectivity		
	H_2/N_2	H_2/CO_2	CO_2/CH_4
PSf - 0	47.11	1.71	30.84
PSf - 10	42.31	1.67	27.55
PSf - 20	36.25	1.53	26.73
PSf - 30	33.58	1.42	25.65

These data indicate that the selectivity of pairs of gases decreases with MgO content. Results suggested that void volume was formed at the interface between polymer and MgO nanoparticles due to the agglomeration of the nanoparticles observed in polymer matrix by SEM.

CONCLUSION

In this study PSf/MgO nanocomposite membranes were prepared succesfully by introducing nanosized MgO particles in a polysulfone polymer network to investigate the effect of nanofiller on the morphology, thermal stability and gas transport properties. The results of the permeation investigation of PSf/MgO nanocomposite membranes show that addition of MgO enhances the gas permeability of polysulfone with increasing nanoparticles content. This behavior results from an increase in free volume because of the inefficient chain packing, as well as the presence of extra void volume at the interface between polymer and MgO nanoparticles.

ACKNOWLEDGEMENTS

The authors are grateful for the financial support provided by the Iran National Science Foundation (INSF) under grant number of 87041855 and Vice President for Research and Technology of Ferdowsi University of Mashhad.

REFERENCES

Ahn, J., Chung, W.-J., Pinnau, I., Guiver, M. D., Polysulfone/silica nanoparticle mixed-matrix membranes for gas separation. Journal Membrane Science, 314, 123-133 (2008).

Arthanareeswaran, G., Thanikaivelan, P., Srinivasn, K., Mohan, D., Rajendran, M., Synthesis, characterization and thermal studies on cellulose acetate membranes with additive. European Polymer Journal, 40, 2153-2159 (2004).

Chatterjee, P. K., Conrad, C. M., Thermo gravimetric analysis of cellulose. Journal Membrane Science, 6, 3217 (1968).

Chung, T.-S., Jiang, L.-Y., Li, Y., Kulprathipanja, S., Mixed matrix membranes (MMMs) comprising organic polymers with dispersed inorganic fillers for gas separation. Prog. Polymer Science, 32, 483-507 (2007).

Cong, H., Radosz, M., Towler, B. F., Shen, Y., Polymer–inorganic nanocomposite membranes for gas separation. Separation and Purification Technology, 55, 281-291 (2007).

Freeman, B. D., Pinnau, I., Polymeric materials for gas separations. ACS Symp. Ser., 733, 1-27 (1999).

George, S. C., Thomas, S., Transport phenomena through polymeric systems. Prog. Polymer Science, 26, 985-1017 (2001).

Gu, F., Wang, Sh.-F., Lu, M.-K., Zou, W.-G., Zhou, G.-J., Xu, D., Yuan, D.-R, Combustion synthesis and luminescence properties of Dy^{3+}-doped MgO nanocrystals. Journal of Crystal Growth, 260, 507-510 (2004).

Han, K. K., Zhou, Y., Chun, Y., Zhu, J. H., Efficient MgO-based mesoporous CO_2 trapper and its performance at high temperature. Journal of Hazardous Materials, 203-204 (2012)

Hosseini, S., Li, Y., Chung, T.-Sh., Liu, Y., Enhanced gas separation performance of nano-composite membranes using MgO nanoparticles. Journal Membrane Science, 302, 207-217 (2007).

Hsu, J. -P., Nacu, A., Preparation of submicron-sized $Mg(OH)_2$ particles through precipitation. Colloids and Surfaces, 262, 220-231 (2005).

Hu, Q., Marand, E., Dhingra, S., Fritsch, D., Wen, J., Wilkes, G., Poly(amideimide)/TiO_2 nanocomposite gas separation membranes, fabrication and characterization. Journal Membrane Science, 135, 65-79 (1997).

Joly, C., Samaihi, M., Porcar, L., Noble, R. D., Polyimide-silica composite materials; how does silica influence their microstructure and gas permeation properties. Chem. Mater., 11, 2331-2338 (1999).

Kim, S., Marand, E., High permeability nano-composite membranes based on mesoporous MCM-41 nanoparticles in a polysulfone matrix. Microporous and Mesoporous Materials, 114 129-136, (2008).

Kim, S. -H., Cho, Ch. -G., Synthesis and characterization of well defined polysulfone-g-poly(styrenesulfonic acid) graft copolymers for proton exchange membrane. Macromolecular Research, v. 19, n. 11, 1142-1150 (2011).

Koros, W. J., Fleming, G. K., Membrane-based gas separation. Journal Membrane Science, 83, 1-80 (1993).

Maier, G., Gas separation with polymer membranes. Angew. Chem. Int. Ed., 37, 2960-2974 (1998).

Mascia, L., Zhang, Z., Shaw, S. -J., Carbon fiber composites based on polyimide/silica creamers, aspects of structure–properties relationship. Com-posites, 27, 1211-1221 (1996).

Matteucci, S., Kusuma, V. A., Kelman, S. D., Freeman, B. D., Gas transport properties of MgO filled poly(1-trimethylsilyl-1-propyne) nanocomposites. Polymer, 49, 1659-1675 (2008).

Matteucci, S., Kusuma, V. A., Sanders, D., Swinnea, S., Freeman, B. D., Gas transport in TiO_2 nanoparticle filled poly(1-trimethylsilyl-1-propyne). Journal Membrane Science, 307,196-217 (2008).

Matteucci, S., Yampol'skii, Y. P., Freeman, B. D., Pinnau, I., Transport of gases and vapors in glassy and rubbery polymers. Materials Science of Membranes for Gas and Vapor Separations. London: John Wiley and Sons, p. 1e48 (2006).

Merkel, T. C., Bondar, V., Nagai, K., Freeman, B. D., Sorption and transport of hydrocarbon and perfluorocarbon gases in poly(1-trimethylsilyl-1-propyne). Journal of Polymer Science, Part B: Polymer Physics, 38, 273-296 (2000).

Moaddeb, M., Koros, W. J., Gas transport properties of thin polymeric membranes in the presence of silicon dioxide particles. Journal Membrane Science, 125, 143-163 (1997).

Moore, T., Koros, W. J., Non-ideal effects in organic–inorganic materials for gas separation membranes. J. Mol. Struct., 739, 87-98 (2005).

Morooka, S., Kusakabe, K., Microporous inorganic membranes for gas separation. MRS Bull, 24, 25-29 (1999).

Okui, T., Saito, Y., Okubo, T., Sadakata, M., Gas permeation of porous organic/inorganic hybrid membranes. J. Sol-Gel Sci., 5, 127-134 (1995).

Pandey, P., Chauhan, R. -S., Membranes for gas separation. Prog. Polym. Sci., 26, 853-893 (2001).

Pavia, D. L., Introduction to Spectroscopy, a Guide for Students of Organic Chemistry. Harcourt Brace College Publishers (1997).

Pollo, L. D., Duarte, L. T., Anacleto, M., Haber, A. C., Borges, C. P., Polymeric membranes containing silver salts for propylene/propane separation. Braz. J. Chem. Eng., v. 29, n. 2, 307-314 (2012).

Rafiq, S., Mana, Z., Maulud, A., Muhammad, N., Maitra, S., Separation of CO_2 from CH_4 using polysulfone/polyimide silica nanocomposite membranes. Separation and Purification, Technology, 90, 162-172 (2012).

Robeson, L. M., Correlation of separation factor versus permeability for polymeric membranes. Journal Membrane Science, 62, 165-185 (1991).

Shi, D., Kong, Y., Yang, J., Du, H., Study on transitional metal organic complex-polyimide hybrid material for gas separation membranes. Acta Polym. Sin., 4, 457- 461 (2000).

Stephen, R., Ranganathaiah, C., Varghese, S., Joseph, K., Thomas, S., Gas transport through nano and micro composites of natural rubber (NR) and their blends with carboxylated styrene butadiene rubber (XSBR) latex membranes. Polymer, 47, 858-870 (2006).

Stern, S. A., Gareis, P. J., Sinclair, T. F., Mohr, P. H., Performance of a versatile variable-volume permeability cell. Comparison of gas permeability measurements by the variable-volume and variable-pressure methods. Journal of Applied Polymer Science, 7, 2035-51 (1963).

Suda, H., Haraya, K., Gas permeation through micropores of carbon molecular sieve membranes derived from Kapton polyimide. J. Phys. Chem. B, 101, 3988-3994 (1997).

Suzuki, T., Yamada, Y., Physical and gas transport properties of novel hyperbranched polyimide-silica hybrid membranes. Polym. Bull., 53, 139-146 (2005).

Te Hennepe, H. J. C., Zeolite filled polymeric membranes, a new concept in separation science. Thesis, University of Twente (1988).

Tin, P. -S., Chung, T. -S., Liu, Y., Wang, R., Liu, S. -L., Pramoda, K. P., Effects of cross-linking modification on gas separation performance of Matrimid membranes. Journal Membrane Science, 225, 77 (2003).

Tsujita, Y., Gas sorption and permeation of glassy polymers with micro voids. Prog. Polym. Sci., 28, 1377 (2003).

Zimmerman, C. M., Singh, A., Koros, W. J., Tailoring mixed matrix composite membranes for gas separations. Journal Membrane Science, 137, 145 (1997).